

# Electrochemical sensing of the thyroid hormone thyronamine (T<sub>0</sub>AM) via molecular imprinted polymers (MIPs)

João G. Pacheco<sup>1</sup>, Patrícia Rebelo<sup>1</sup>, Fernando Cagide<sup>2</sup>, Luís Moreira Gonçalves<sup>\*,3,4</sup>, Fernanda Borges<sup>2</sup>, José António Rodrigues<sup>3</sup>, Cristina Delerue-Matos<sup>1</sup>

<sup>1</sup>REQUIMTE/LAQV, Instituto Superior de Engenharia do Porto (ISEP), Politécnico do Porto, Rua Dr. António Bernardino de Almeida 431, 4200-072 Porto, Portugal

<sup>2</sup>CIQUP, Departamento de Química e Bioquímica, Faculdade de Ciências, Universidade do Porto (FCUP), Rua do Campo Alegre, s/n, 4169-007, Porto, Portugal

<sup>3</sup>REQUIMTE/LAQV, Departamento de Química e Bioquímica, Faculdade de Ciências, Universidade do Porto (FCUP), Rua do Campo Alegre, s/n, 4169-007, Porto, Portugal

<sup>4</sup>Departamento de Química Fundamental, Instituto de Química, Universidade de São Paulo (USP), Av. Prof. Lineu Prestes, 748 - Butantã, 05508-000 São Paulo, SP, Brazil

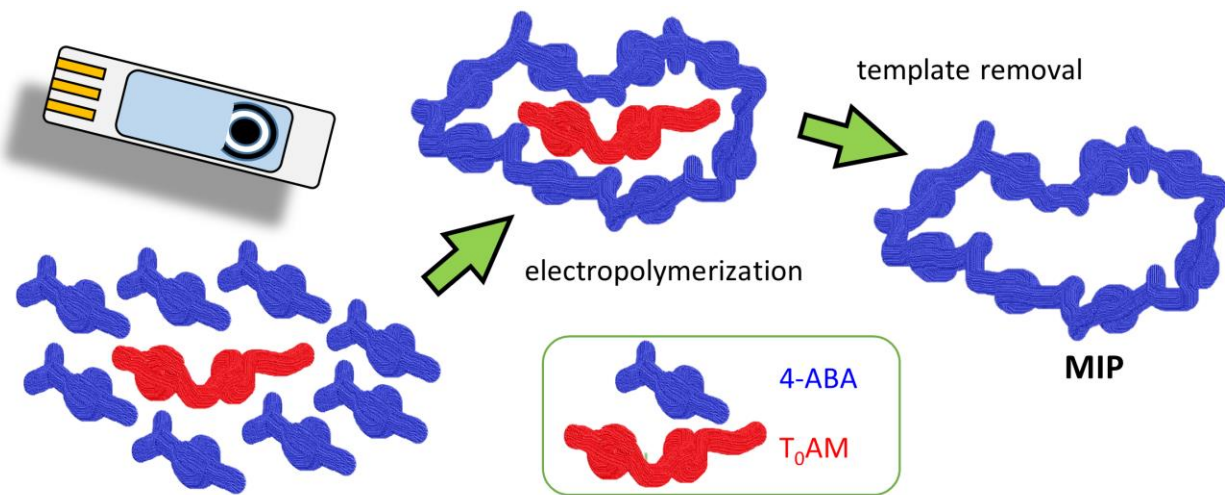
\*Corresponding author: address: B5 térreo, sala 519, Departamento de Química Fundamental, Instituto de Química, Universidade de São Paulo (USP), Avenida Prof. Lineu Prestes, 748, Vila Universitária, São Paulo - SP, 05508-000, Brasil; phone number: +55 11 3091 2165; e-mail: lmgoncalves@iq.usp.br

## ABSTRACT

Recent studies have shown that besides the well-known T<sub>3</sub> (triiodothyronine) and T<sub>4</sub> (thyroxine) there might be other important thyroid hormones, in particular T<sub>0</sub>AM (thyronamine) and T<sub>1</sub>AM (3-iodothyronamine). The absence of a large number of studies showing their precise importance might be explained by the limited number of analytical methodologies available. This work aims to show an electroanalytical alternative making use of electropolymerized molecularly imprinted polymer (MIPs). The MIPs' polymerization is performed on the surface of screen-printed carbon electrodes (SPCEs), using 4-aminobenzoic acid (4-ABA) as the building and functional monomer and the analyte T<sub>0</sub>AM as the template. The step-by-step construction of the SPCE-MIP sensor was studied by cyclic voltammetry (CV) and by electrochemical impedance spectroscopy (EIS). After optimization, by means of square-wave voltammetry, the SPCE-MIP showed suitable selectivity (in comparison with other thyroid hormones and catechol amines), repeatability (intra-day of 3.9%), a linear range up to 10 μmol L<sup>-1</sup> (0.23 x 10<sup>3</sup> μg dL<sup>-1</sup>) with an r<sup>2</sup> of 0.998 and a limit of

detection (LOD) and quantification (LOQ) of 0.081 and 0.27  $\mu\text{mol L}^{-1}$  (1.9 and 6.2  $\mu\text{g dL}^{-1}$ ), respectively.

Graphical Abstract:



### Keywords:

Electroanalysis; Electropolymerization; Endocrinology; Modified working electrode; Molecular recognition; Poly(para-aminobenzoic acid) film.

## 1. Introduction

Thyroid hormones are relevant actors in several physiological roles, including, but not limited to, metabolism and thermogenesis. Although T<sub>1</sub>AM (3-iodothyronamine) and T<sub>0</sub>AM (thyronamine) were already known for many decades, only 15 years ago studies started to appear revealing an unexpected biological significance [1]. Both T<sub>1</sub>AM and T<sub>0</sub>AM appear to induce transient hypothermia and marked neuroprotection against injuries caused by stroke [2]. T<sub>0</sub>AM seems also to influence cardiac output, heart rate and to be relevant in many other metabolic roles; indeed the idea that T<sub>1</sub>AM and T<sub>0</sub>AM, like T<sub>3</sub> (triiodothyronine) and T<sub>4</sub> (thyroxine), have their own significant physiological importance seems now to be supported by several studies [1,3–6]. Nevertheless, there are many questions that remain unanswered, e.g. their endogenous levels are still largely unknown [7]. In this context novel simple and quick analytical options can make a difference.

The selective extraction of the analytes is a sample preparation techniques that can greatly influence an analytical methodology, to an extent of sometimes making it possible [8].

Molecularly imprinted polymers (MIPs) were imagined as a lab-made alternative to biological receptors, imitating antibodies [9], MIPs have tailor-made selective recognition sites for selected molecules [10–12]. These biomimetic polymers are obtained by polymerization, a process in which the building monomers are polymerized around a target template (generally, the aimed analyte). This polymerization can be electrochemical (electropolymerization) [13] and can be performed directly on the screen-printed electrode surface [14]. Subsequent to polymerization, the template molecule is extracted and a polymer matrix, with sites complementary in size and shape, to the analyte, is obtained. Although there can be found in literature a few works with MIPs developed for T<sub>4</sub> [15,16], authors are not aware of any similar developments for T<sub>0</sub>AM. Electrochemical MIP-based sensors combine the advantages of MIPs (mainly their selectivity) with the advantages inherent to electrochemical sensors namely: portability, speed of analysis, user-friendliness, simplicity and sensitivity [17], these can be powerful tools for point-of-care applications [18–20].

There are not many analytical methodologies for T<sub>0</sub>AM [21,22], and, to best of our knowledge, no electroanalytical methodologies, although there is a first original work showing that T<sub>0</sub>AM is electrochemically active and that can be oxidized on a glassy carbon electrode (GCE) [23]. Köhrle and co-workers recently published a liquid-liquid extraction/isotope dilution-liquid chromatography-electrospray tandem mass spectrometry (LC-MS) methodology that simultaneously analyzed several thyroid hormones. It achieved a LOD of 0.13 nmol L<sup>-1</sup> in human hepatocellular carcinoma Hep G2 cell lysate extracts [21]. The same group had previously developed a different LC-MS/MS in cell culture media with a very low LOD of 0.06 nmol L<sup>-1</sup> [22]. Recently, Li *et al.* developed a LC-MS methodology for the determination of thyroid hormones in placenta, however they did not to determine T<sub>0</sub>AM [24].

In this work a voltammetric MIP sensor was developed for the analysis of T<sub>0</sub>AM. The MIP was produced by electropolymerization on the surface of a screen-printed carbon electrode (SPCE). These developments may aid the development of a point-of-care alternative for T<sub>0</sub>AM which may help endocrinologists to fully understand this hormone's protagonism within the complex thyroid puzzle.

## 2. Experimental

### 2.1. Chemicals and general conditions

All commercial reagents used were of analytical grade and were used without further purification. Triiodothyronine (T<sub>3</sub>) and thyroxine (T<sub>4</sub>), potassium hexacyanoferrate (III), potassium

hexacyanoferrate (II) trihydrate (the pair  $[\text{Fe}(\text{CN})_6]^{3-/4-}$ ), 4-aminobenzoic acid (4-ABA), hydrochloric acid, tert-butyl (4-hydroxyphenethyl)carbamate, (4-(methoxymethoxy)phenyl)boronic acid, copper (II) acetate, pyridine, epinephrine, norepinephrine, dopamine, triethylamine, trifluoroacetic acid and molecular sieves 4 Å were purchased from Sigma-Aldrich, methanol was purchased from Merck. Phosphate buffer solution (PBS), 0.1 mol L<sup>-1</sup>, pH 7.4 was prepared with potassium dihydrogen phosphate (KH<sub>2</sub>PO<sub>4</sub>) and potassium hydrogen phosphate (K<sub>2</sub>HPO<sub>4</sub>), both from Riedel-de-Haën.

Ultrapure water (resistivity not less than 18.2 Ω cm at 298 K) from a Direct-Q 3UV water purification system (Millipore) was used in all experiments. Thin-layer chromatography (TLC) was carried out on precoated silica gel 60 F254 (Merck) with layer thickness of 0.2 mm. For analytical control the following systems were used: ethyl acetate/petroleum ether, methanol/dichloromethane in several proportions. The spots were visualized under UV detection (254 and 366 nm). Flash chromatography was performed using silica gel 60 0.2-0.5 or 0.040-0.063 mm (Carlo Erba Reagents).

Stock solutions of T<sub>0</sub>AM (50 mmol L<sup>-1</sup>) were prepared in PBS and stored at 4 °C. Freshly working solutions, with different concentrations, were prepared each day through dilution of the previous one, making use of the same buffer.

## **2.2. Equipment**

Nuclear magnetic resonance (NMR) spectra were acquired, at room temperature, on a Brüker AMX 400 spectrometer operating at 400.15 MHz for <sup>1</sup>H and 100.62 MHz for <sup>13</sup>C. Chemical shifts were expressed in δ (ppm) values relative to tetramethylsilane (TMS) as internal reference; coupling constants (*J*) were given in Hz. Assignments were also made from DEPT (Distortionless Enhancement by Polarization Transfer) (underlined values).

Voltammetric measurements, such as cyclic voltammetry (CV) and square wave voltammetry (SWV), were carried out using an Autolab PGSTAT 204 potentiostat/galvanostat (Metrohm Autolab) and electrochemical impedance spectroscopic (EIS) analysis were performed using an Autolab PGSTAT 128N (Metrohm Autolab). The equipment was controlled by NOVA software (version 1.11, Metrohm Autolab). Screen-printed carbon electrodes (SPCE, DropSens, DRP-110) with carbon working (d = 4.0 mm) and auxiliary electrodes and a silver (Ag) reference electrode were used.

### 2.3. Chemical synthesis

4-(4-(2-Aminoethyl)phenoxy)phenol ( $T_0AM$ ) and 4-(4-(2-aminoethyl)-2-iodophenoxy)phenol ( $T_1AM$ ) were synthesized from *tert*-butyl (4-hydroxyphenethyl)carbamate (**1**) following the synthetic strategies shown in Fig. 1.

The compounds were obtained in moderate to high yields and fully characterized by magnetic resonance spectroscopy ( $^1H$ RMN,  $^{13}C$ RMN and DEPT135). The purity of the final products (> 97% purity) was verified by NMR and High-performance liquid chromatography with diode array detection (HPLC-DAD), equipped with a commercially prepacked Waters Spherisorb RP-18 (5  $\mu$ m) ODS2 column, with 4.6 mm internal diameter and 250 mm length, and a Waters 996 PDA detector at the maximum wavelength of 254 nm. The mobile phase consisted of methanol [0.05% trifluoroacetic acid (TFA)]/water (gradient elution, room temperature) at a flow rate of 1 mL min $^{-1}$ .

All RMN spectra are present in the Supporting Information.

#### 2.3.1. Synthesis of 4-(4-(2-aminoethyl)phenoxy)phenol ( $T_0AM$ )

Step 1 - To a solution of *tert*-butyl (4-hydroxyphenethyl)carbamate (**1**) (200 mg, 0.84 mmol) and (4-(methoxymethoxy)phenyl)boronic acid (307 mg, 1.69 mmol) in anhydrous dichloromethane (8 mL) under argon atmosphere activated molecular sieves 4 Å (1 g) were added. The reaction was stirred for 10 minutes and then copper (II) acetate (153 mg, 0.84 mmol), pyridine (341  $\mu$ L, 4.21 mmol) and triethylamine (578  $\mu$ L, 4.21 mmol) were added. The reaction was stirred overnight at ambient temperature. After diethyl ether was added and the formed solid was removed by filtration. The organic solution was washed with hydrochloric acid 1 mol L $^{-1}$  and water and dried over sodium sulphate. After solvent evaporation the crude product was purified by flash chromatography (ethyl acetate/petroleum ether). *tert*-Butyl (4-(4-(methoxymethoxy)phenoxy)phenethyl)carbamate (**2**) was obtained as a white solid (220 mg, 70% yield). In the copper mediated coupling of a boronic acid with the appropriate protected phenol there no ortho-coupling takes place [25,26].

$^1H$  NMR (400 MHz,  $CDCl_3$ ): 7.15 – 7.08 (H3,H5, m, 2H), 7.04 – 6.99 (H2', H6', m, 2H), 6.97 – 6.92 (H2, H3, m, 2H), 6.92 – 6.87 (H3', H5', m, 2H), 5.15 (OCH $_2$ O, s, 2H), 4.54 (NH, bs, 1H), 3.50 (OCH $_3$ , s, 3H), 3.35 (H8, dt,  $J$  = 7.0, 6.0 Hz, 2H), 2.75 (H7, t,  $J$  = 7.0 Hz, 2H), 1.44 (OC(CH $_3$ ) $_3$ , s, 9H).

<sup>13</sup>C NMR (101 MHz, CDCl<sub>3</sub>): 156.8 (NHCOO), 155.9 (C4), 153.4 (C4'), 151.5 (C1'), 133.2 (C1), 129.9 (C2, C6), 120.4 (C2', C6'), 118.1 (C3, C5), 117.6 (C3', C5'), 95.1 (OCH<sub>2</sub>O), 79.3 (OC(CH<sub>3</sub>)<sub>3</sub>), 56.0 (OCH<sub>3</sub>), 41.9 (C8), 35.5 (C7), 28.4 (OC(CH<sub>3</sub>)<sub>3</sub>).

Step 2 - *Tert*-Butyl (4-(4-(methoxymethoxy)phenoxy)phenethyl)carbamate (**2**) (210 mg, 0.56 mmol) was dissolved in methanol (2 mL) and concentrated hydrochloric acid (200 μL) was added. The reaction was stirred at 65 °C for 3 hours. Then, it was neutralized with a saturate solution of sodium hydrogen carbonate and extracted with ethyl acetate. The combined organic phases were dried over sodium sulphate and the solvent was evaporated. The crude product was purified by flash chromatography (methanol/ dichloromethane). T<sub>0</sub>AM was obtained as a white solid (46 mg, 36% yield).

<sup>1</sup>H NMR (400 MHz, MeOD): 7.24 – 7.11 (H3, H5, m, 2H), 6.87 – 6.80 (H2, H6, H2', H6', m, 4H), 6.80 – 6.74 (H3', H5', m, 1H), 2.87 (H8, t, *J* = 7.2 Hz, 1H), 2.72 (H7, t, *J* = 7.2 Hz, 1H).

<sup>13</sup>C NMR (101 MHz, MeOD): 158.8 (C4), 154.9 (C4'), 150.7 (C1'), 134.5 (C1), 130.9 (C2, C6), 121.8 (C2', C6'), 118.5 (C3, C5), 117.2 (C3', C5'), 44.1 (C8), 38.8 (C7).

### 2.3.2. Synthesis of 4-(4-(2-aminoethyl)-2-iodophenoxy)phenol (T<sub>1</sub>AM)

Step 1 - *tert*-Butyl (4-hydroxy-3-iodophenethyl)carbamate (**3**) was obtained following a procedure described in the literature [27]. The spectral data was in accordance with the assigned structure.

Step 2 - To a solution of *tert*-butyl (4-hydroxy-3-iodophenethyl)carbamate (**3**) (308 mg, 0.84 mmol) and (4-(methoxymethoxy)phenyl)boronic acid (306 mg, 0.84 mmol) in anhydrous dichloromethane (8 mL) under argon atmosphere activated molecular sieves 4 Å (1 g) were added. The reaction mixture was stirred for 10 minutes and then copper (II) acetate (153 mg, 0.84 mmol), pyridine (341 μL, 4.21 mmol) and triethylamine (578 μL, 4.21 mmol) were added. The reaction was stirred overnight at ambient temperature and then diethyl ether was added and the formed solid was removed by filtration. The organic solution was washed with hydrochloric acid 1 mol L<sup>-1</sup> and water and dried over sodium sulphate. The solvent was evaporated, and the crude product was purified by flash chromatography (ethyl acetate/petroleum ether). *tert*-Butyl (3-iodo-4-(4-(methoxymethoxy)phenoxy)phenethyl)carbamate (**4**) was obtained as a white solid (314 mg, 74 % yield).

$^1\text{H}$  NMR (400 MHz,  $\text{CDCl}_3$ ): 7.67 (H2, d,  $J = 2.1$  Hz, 1H), 7.07 (H6, dd,  $J = 8.3, 2.1$  Hz, 1H), 7.04 – 6.99 (H2', H6', m, 2H), 6.94 – 6.89 (H3', H5', m, 2H), 6.73 (H5, d,  $J = 8.3$  Hz, 1H), 5.14 (OCH<sub>2</sub>O OCH<sub>2</sub>O s, 2H), 4.56 (NH, bs, 1H), 3.49 (OCH<sub>3</sub>, s,  $J = 2.2$  Hz, 3H), 3.41 – 3.28 (H8, 2H), 2.73 (H7, t,  $J = 7.0$  Hz, 2H), 1.44 (OC(CH<sub>3</sub>)<sub>3</sub>, s, 9H).

$^{13}\text{C}$  NMR (101 MHz,  $\text{CDCl}_3$ ): 155.9 (NHCOO), 155.8 (C4), 153.5 (C4'), 151.3 (C1'), 139.8 (C2), 135.8 (C1), 129.9 (C6), 120.0 (C2', C6'), 118.2 (C5), 117.6 (C3', C5'), 95.0 (OCH<sub>2</sub>O), 88.2 (C3), 79.4 (OC(CH<sub>3</sub>)<sub>3</sub>), 56.0 (OCH<sub>3</sub>), 41.7 (C8), 35.0 (C7), 28.4 (OC(CH<sub>3</sub>)<sub>3</sub>).

Step 3 - *tert*-Butyl (3-iodo-4-(4-(methoxymethoxy)phenoxy)phenethyl)carbamate (**4**) (256 mg, 0.57 mmol) was dissolved in methanol (5 mL) and concentrated HCl (400  $\mu\text{L}$ ) was added. The reaction was stirred at 65 °C for 3 hours. Then, it was neutralized with a saturate solution of sodium hydrogen carbonate. The formed solid was filtered, washed with water and dried. T<sub>1</sub>AM was obtained as a white solid (156 mg, 77% yield).

$^1\text{H}$  NMR (400 MHz, MeOD): 7.71 (H2, d,  $J = 2.1$  Hz, 1H), 7.13 (H6, dd,  $J = 8.3, 2.1$  Hz, 1H), 6.82 – 6.73 (H2', H3', H5', H6', m, 4H), 6.68 (H5, d,  $J = 8.3$  Hz, 1H), 2.85 (H8, t,  $J = 7.2$  Hz, 2H), 2.69 (H7, t,  $J = 7.2$  Hz, 2H).

$^{13}\text{C}$  NMR (101 MHz, MeOD): 157.8 (C4), 155.1 (C4'), 150.7 (C1'), 140.9 (C2), 137.4 (C1), 131.1, 121.2 (C2', C6'), 118.7 (C5), 117.2 (C3', C5'), 88.3 (C3), 44.0 (C8), 38.5 (C7).

#### 2.4. MIP/NIP construction

Prior to modification, the bare SPCE were rinsed with water and activated with sulphuric acid, 0.1 mol L<sup>-1</sup>, using cycling voltammetry (CV), for 5 cycles, at 100 mV s<sup>-1</sup> between -0.2 V and +1.3 V. The MIP-sensor was obtained by electropolymerization on the surface of the SPCE by applying 10 CV scans in the potential range between -0.2 V and +1.4 V, at a scan rate of 100 mV s<sup>-1</sup>.

The polymerization solution included the template molecule T<sub>0</sub>AM, 1 mmol L<sup>-1</sup>, and monomer 4-ABA, 10 mmol L<sup>-1</sup>, prepared in hydrochloric acid, 0.1 mol L<sup>-1</sup>; 40  $\mu\text{L}$  of this solution were dropped on the electrode (this was the minimum volume that permitted to cover the three electrodes). The NIP-sensor was also prepared under the same polymerization conditions but without adding the template molecule. Then, the electrodes were rinsed with water before proceeding.

After the electropolymerization process, 40  $\mu\text{L}$  of a methanol/hydrochloric acid, 1 mol L<sup>-1</sup>, (50:50, v/v) solution was placed and replaced each 5 minutes on the sensor surface during 20

minutes. This procedure had the goal of removing of the entrapped T<sub>0</sub>AM molecules inside the polymeric film thus creating the specific binding cavities.

## 2.5. Electrochemical measurements

The electrochemical response of T<sub>0</sub>AM at the modified electrode under the optimum conditions was performed by SWV, through a simple procedure. All measurements were performed at room temperature. Initially, the prepared modified electrodes were incubated with 40 µL of the T<sub>0</sub>AM solutions during 8 minutes. Then, the sensor was washed briefly with water and dried, and was transferred to a specific connector for the analysis of the T<sub>0</sub>AM binding to by SWV (from -0.2 to +0.8 V with a step potential of 5 mV, wave amplitude of 20 mV and frequency of 25 Hz in PBS). This means that the SWV measurements were performed on the T<sub>0</sub>AM that bound to the MIPs during the incubation time. The selectivity studies were performed in a similar manner.

EIS measurements, performed in the characterization studies, were done by using a sinusoidal signal of amplitude 10 mV, with frequency range from 10 mHz to 0.1 MHz and fixed electrical potential of 0.2 V. The CV (scan rate of 100 mV s<sup>-1</sup>, from -0.2 to +0.6 V) and EIS characterization analysis of SPCE -non-imprinted polymer (NIP) and -MIP sensor were conducted with a 40 µL of PBS and 2 mmol L<sup>-1</sup> of [Fe(CN)<sub>6</sub>]<sup>3-/4-</sup>, respectively.

## 3. Results and discussion

### 3.1. Chemical synthesis

T<sub>0</sub>AM and T<sub>1</sub>AM were obtained following the synthetic strategies described in Fig. 1. Even though the approaches were based on a previously described one [25], in this work the number of steps was reduced by the use of watchful chosen starting materials and phenol and amine protecting groups (methoxymethyl ether (MOM) *tert*-butyloxycarbonyl (BOC)).

T<sub>0</sub>AM was synthesized by a two-step strategy that comprised the coupling of *tert*-butyl (4-hydroxyphenethyl)carbamate (**1**) with (methoxymethoxy)phenylboronic acid via a copper(II)-mediated process giving the diphenyl ether compound **2**. Afterwards, compound **2** was submitted to a deprotection process of the phenol and amine protecting groups with hydrochloric acid in methanol and compound T<sub>0</sub>AM was obtained.



T<sub>1</sub>AM was synthesized by a similar synthetic strategy using compound **3** as starting material, which was obtained by the iodination of *tert*-butyl (4-hydroxyphenethyl)carbamate **1**. The subsequent coupling process with the (methoxymethoxy)phenyl)boronic acid produce compound **4** that after a subsequent deprotection process with hydrochloric acid provided the desired compound T<sub>1</sub>AM.

### 3.2. Sensor development and characterization

The overall process of the development of the SPCE-MIP sensor is schematized in Fig. 2: it consists on electropolymerization of the building monomer around the template; removal of template leaving being cavities suited for the analyte; and selective analysis, i.e. only the analyte should adequately fit within the molded cavities. The electropolymerization was performed with 4-ABA on the electrode surface, by CV, using the analyte T<sub>0</sub>AM as the template and using 4-ABA in a dual role of both the building monomer and the functional monomer. 4-ABA is a good monomer for electropolymerization since not only it can be easily electropolymerized (to a poly(4-aminobenzoic acid) film) on various substrate materials but also because it form films with good coverage [28,29] and suitable chemical template [11,30–33]. In the electrodeposition process, the T<sub>0</sub>AM template molecules are entrapped within the MIP. One can suggest that there are reasonably strong interactions due to hydrogen bonds between the amino and the hydroxyl group from the T<sub>0</sub>AM with both the carboxyl group and the amino group of 4-ABA units from the poly(4-aminobenzoic acid) film, and, quite possibly some  $\pi$ - $\pi$  stacking between the aromatic structures of both compounds [30].

During each step of the construction of the SPCE-MIP sensor, it was characterized by CV and EIS using 2 mmol L<sup>-1</sup> [Fe(CN)<sub>6</sub>]<sup>3-/4-</sup> (Fig. 3). In the EIS, the smaller semi-circle of the Nyquist diagram (minor resistance) corresponds to the bare SPCE. Then, the charge transfer to the ferricyanide/ferrocyanide couple decreases with the electropolymerization, both from the MIP and NIP (the diameter of the semi-circle enlarged), though the NIP seems to be a better conductor than the MIP. After removing the template, charge transfer increases again, though not to the initials levels of the bare SPCE, which might be clarified by the formation of cavities improving diffusion. After incubation, the resistance to the electron flow increases, but also not to the levels of the electropolymerization. This indicates a successful analyte entrapment by the MIP. A similar behavior was observed in the CV analysis. Two well defined peaks were observed for the unmodified SPCE. The signal decreases with both MIP and NIP electropolymerization with an

association increase in the peak-to-peak potential, showing that the diffusional electron transfer is harmed. Then it increases with the template removal and decreases slightly with the analyte incubation. In these characterization studies the electrochemical signal arose from the ferrocyanide redox probe [34], present at a meaningful concentration, and not the analyte itself, however that is not the case for the following experiments since the T<sub>0</sub>AM was itself electrochemically active [23].

Several parameters in the preparation of the MIPs had to be optimized, namely: monomer concentration, template concentration, incubation time and solvent of extraction (Fig. 4). It was observed that, up to a certain point, there was a signal increase with larger concentrations of the building monomer 4-ABA. The final 4-ABA concentration chosen for the MIP synthesis was 10 mmol L<sup>-1</sup> (Fig. 4 - A). Then, the template concentration was optimized, the optimal value was 1 mmol L<sup>-1</sup>, larger concentrations seem not increase any signal (Fig. 4 - B). Subsequently, the incubation time was optimized. Signal increment after 10 minutes was not meaningful enough to delay the analysis (Fig. 4 - C). Finally, solvent extraction was optimized. The removal of the template is of the utmost importance; the solvent has to be effective on removing the template without compromising MIP stability. Of all the solvents and mixtures tested (water, methanol, hydrochloric acid, sodium hydroxide, hydrochloric acid/methanol and water/dimethyl sulfoxide [31]), the best result was obtained with hydrochloric acid/methanol. Removal may arise from strong hydrogen bonds that methanol creates with the template in an acidic value of pH.

Observing the electropolymerization it is clear that the current decreases along the polymerization process, and that the NIP polymerization, in comparison with the MIP polymerization, produces lower currents (figures of this process are present in the Supporting Information) [35]. Figure 5 - A shows that there is a well-defined peak before the template extraction that subsequently disappears, i.e. solvent extraction seems to be efficient. Figure 5 - B shows that there is no T<sub>0</sub>AM adsorption to the unmodified SPCE or, if there is some, considering a possible  $\pi$ - $\pi$  interaction between the aromatic groups from the analyte and the carbonic surface [34,36], it is minimal. It also shows that there is a minimum binding of T<sub>0</sub>AM to the NIP when compared with the MIP. This corroborates the assumption that the electroanalytical signal is due the T<sub>0</sub>AM within the MIP [31].

### 3.3. Analytical parameters

The selectivity of the developed MIPs was studied in a comparison with other compounds (further thyroid hormones, and common catechol amines), the obtained results are summarized in Table 1. For each compound it was calculated the imprinting factor (IF) that was determined using the following equation:

$$1) \quad IF = \frac{i_p(MIP)}{i_p(NIP)}$$

Where  $i_p$  is the peak current, which means IF should be above 1.0 and as high as possible. After obtaining the IF, it was possible to calculate the specific selectivity factor ( $\alpha$ ) using the following equation.

$$2) \quad \alpha = \frac{IF_{T_0AM}}{IF_{interferent}}$$

Which, obviously, should also be above 1.0 and as high as possible. The obtained results displayed in Table 1, show that the sensor was quite selective. In particular, it should be mentioned that the selectivity studies were performed with very similar molecules, both in size and in terms of functional groups, that are commonly present in the same fluids. These results demonstrate that the recognition sites formed in the polymerized film have the capability to discriminate the analyte through a combination of their size, shape and functional group distribution [30].

The corresponding calibration curve ( $n = 9$ ) had the following analytical parameters (Fig. 6): a  $r^2$  of 0.998,  $i_p (A) = (306.2 \pm 5.1) \times [T_0AM] \text{ (mmol L}^{-1}\text{)} + (1.5 \pm 2.5) \times 10^{-8}$ , limit of detection (LOD) and quantification (LOQ) of 0.081 and 0.27  $\mu\text{mol L}^{-1}$  (1.9 and 6.2  $\mu\text{g dL}^{-1}$ ), respectively, with a linear range of up to 10  $\mu\text{mol L}^{-1}$  ( $2.3 \times 10^2 \mu\text{g dL}^{-1}$ ). LOD and LOQ were calculated as three and ten times the standard deviation of the intercept divided by the slope [37], respectively. Each sensor was re-used about 10 times without any change in signal. The intra-day repeatability was 3.9% and the inter-day repeatability was of 10.0% (both evaluated by measuring a solution of 1  $\mu\text{mol L}^{-1}$ ).

To the best of our knowledge, not only this is the first time MIPs were developed to T<sub>0</sub>AM but it is also the first electroanalytical alternative for T<sub>0</sub>AM, having its typical advantages when compared to LC-MS methodologies, like portability, simplicity, low-cost, lower time of analysis and solvent economization [38].

## 4. Conclusions

This work successfully showed that it is possible to develop a SPCE-MIP sensor for the electrochemical analysis of T<sub>0</sub>AM. Both the analyte (T<sub>0</sub>AM) and one of the possible interferences studied (T<sub>1</sub>AM) had to be synthesized since they are not commercially available. A poly(4-aminobenzoic acid) film was created by electropolymerization of the monomer 4-ABA to adequately have gaps to which the T<sub>0</sub>AM can suitably physico-chemically fit. The SPCE-MIP sensor characterized by EIS showing and adequate MIP formation and suitable binding with the analyte. The developed sensor SPCE showed appropriate analytical parameters and selectivity in comparison with relevant compounds.

## Acknowledgements

This project was supported by Fundação para a Ciência e a Tecnologia (FCT), and FEDER/COMPETE (UID/QUI/00081/2013, UID/QUI/50006/2013, POCI-01-0145-FEDER-006980 and NORTE-01-0145-FEDER-000028), JGP (SFRH/BPD/101419/2014), PR (SFRH/BD/132384/2017) and LMG (SFRH/BPD/76544/2011) wish to acknowledge FCT for their research grants. FC thanks NORTE-01-0145-FEDER-000028 grant.

All authors declare no conflicts of interest.

## References

- [1] S. Piehl, C.S. Hoefig, T.S. Scanlan, J. Köhrle, Thyronamines—Past, Present, and Future, *Endocr. Rev.* 32 (2011) 64–80. doi:10.1210/er.2009-0040.
- [2] K.P. Doyle, K.L. Suchland, T.M.P. Ciesielski, N.S. Lessov, D.K. Grandy, T.S. Scanlan, M.P. Stenzel-Poore, Novel Thyroxine Derivatives, Thyronamine and 3-iodothyronamine, Induce Transient Hypothermia and Marked Neuroprotection Against Stroke Injury, *Stroke*. 38 (2007) 2569–2576. doi:10.1161/STROKEAHA.106.480277.
- [3] T.S. Scanlan, K.L. Suchland, M.E. Hart, G. Chiellini, Y. Huang, P.J. Kruzich, S. Frascarelli, D.A. Crossley, J.R. Bunzow, S. Ronca-Testoni, E.T. Lin, D. Hatton, R. Zucchi, D.K. Grandy, 3-Iodothyronamine is an endogenous and rapid-acting derivative of thyroid hormone, *Nat. Med.* 10 (2004) 638–642. doi:10.1038/nm1051.
- [4] G. Rutigliano, R. Zucchi, Cardiac actions of thyroid hormone metabolites, *Mol. Cell. Endocrinol.* 458 (2017) 76–81.

doi:10.1016/j.mce.2017.01.003.

- [5] R. Senese, F. Cioffi, P. de Lange, F. Goglia, A. Lanni, Thyroid: biological actions of “nonclassical” thyroid hormones, *J. Endocrinol.* 221 (2014) R1–R12. doi:10.1530/JOE-13-0573.
- [6] R.A.S. Couto, L.M. Gonçalves, M.S. Góes, C.M.P. Rodrigues, M.B. Quinaz, J.A. Rodrigues, SAM-Based Immunosensor for the Analysis of Thyroxine (T4), *J. Electrochem. Soc.* 164 (2017) B103–B106. doi:10.1149/2.0561704jes.
- [7] G. Chiellini, L. Bellusci, M. Sabatini, R. Zucchi, Thyronamines and Analogues - The Route from Rediscovery to Translational Research on Thyronergic Amines, *Mol. Cell. Endocrinol.* 458 (2017) 149–155. doi:10.1016/j.mce.2017.01.002.
- [8] L.M. Gonçalves, I.M. Valente, J.A. Rodrigues, Recent Advances in Membrane-Aided Extraction and Separation for Analytical Purposes, *Sep. Purif. Rev.* 46 (2017) 179–194. doi:10.1080/15422119.2016.1235050.
- [9] C.R.T. Tarley, M.D.P.T. Sotomayor, L.T. Kubota, Polímeros biomiméticos em química analítica. Parte 1: preparo e aplicações de MIP (“Molecularly Imprinted Polymers”) em técnicas de extração e separação, *Quim. Nova.* 28 (2005) 1076–1086. doi:10.1590/S0100-40422005000600024.
- [10] G.A. Ruiz-Córdova, S. Khan, L.M. Gonçalves, M.I. Pividori, G. Picasso, M.D.P.T. Sotomayor, Electrochemical sensing using magnetic molecularly imprinted polymer particles previously captured by a magneto-sensor, *Talanta.* 181 (2018) 19–23. doi:10.1016/j.talanta.2017.12.085.
- [11] S. Khan, S. Hussain, A. Wong, M.V. Foguel, L. Moreira Gonçalves, M.I. Pividori Gurgo, M. del P. Taboada Sotomayor, Synthesis and characterization of magnetic-molecularly imprinted polymers for the HPLC-UV analysis of ametryn, *React. Funct. Polym.* 122 (2018) 175–182. doi:10.1016/j.reactfunctpolym.2017.11.002.
- [12] A.N. Baeza-Fonte, I. Garcés-Lobo, M.D. Luaces-Alberto, L.M. Gonçalves, M.D.P.T. Sotomayor, A.C. Valdés-González, Determination of Cephalosporins by UHPLC-DAD Using Molecularly Imprinted Polymers, *J. Chromatogr. Sci.* 56 (2018) 187–193. doi:10.1093/chromsci/bmx099.
- [13] C. Zhong, B. Yang, X. Jiang, J. Li, Current Progress of Nanomaterials in Molecularly Imprinted Electrochemical Sensing, *Crit. Rev. Anal. Chem.* 48 (2018) 15–32. doi:10.1080/10408347.2017.1360762.
- [14] D.-M. Kim, J.-M. Moon, W.-C. Lee, J.-H. Yoon, C.S. Choi, Y.-B. Shim, A potentiometric non-enzymatic glucose sensor using a molecularly imprinted layer bonded on a conducting polymer, *Biosens. Bioelectron.* 91 (2017) 276–283. doi:10.1016/j.bios.2016.12.046.
- [15] B.B. Prasad, M.P. Tiwari, R. Madhuri, P.S. Sharma, Enantioselective quantitative separation of d- and l-thyroxine by molecularly imprinted micro-solid phase extraction silver fiber coupled with complementary molecularly imprinted polymer-sensor, *J. Chromatogr. A.* 1217 (2010) 4255–4266. doi:10.1016/j.chroma.2010.04.055.
- [16] S.L. Moura, L.M. Fajardo, L. dos A. Cunha, M.D.P.T. Sotomayor, F.B.C. Machado, L.F.A. Ferrão, M.I. Pividori, Theoretical and experimental study for the biomimetic recognition of levothyroxine hormone on magnetic molecularly imprinted polymer, *Biosens. Bioelectron.* 107 (2018) 203–210. doi:10.1016/j.bios.2018.01.028.
- [17] M.M. Pedroso, M.V. Foguel, D.H.S. Silva, M. del P.T. Sotomayor, H. Yamanaka, Electrochemical sensor for dodecyl gallate determination based on electropolymerized molecularly imprinted polymer, *Sensors Actuators B Chem.* 253 (2017) 180–186. doi:10.1016/j.snb.2017.06.127.
- [18] B.V.M. Silva, B.A.G. Rodríguez, G.F. Sales, M.D.P.T. Sotomayor, R.F. Dutra, An ultrasensitive human cardiac troponin T graphene screen-printed electrode based on electropolymerized-molecularly imprinted conducting polymer, *Biosens. Bioelectron.* 77 (2016) 978–985. doi:10.1016/j.bios.2015.10.068.
- [19] G. Maduraiveeran, M. Sasidharan, V. Ganesan, Electrochemical sensor and biosensor platforms based on advanced nanomaterials for biological and biomedical applications, *Biosens. Bioelectron.* 103 (2018) 113–129. doi:10.1016/j.bios.2017.12.031.
- [20] J.G. Pacheco, M.S.V. Silva, M. Freitas, H.P.A. Nouws, C. Delerue-Matos, Molecularly imprinted electrochemical sensor for the point-of-care detection of a breast cancer biomarker (CA 15-3), *Sensors Actuators B Chem.* 256 (2018) 905–912. doi:10.1016/j.snb.2017.10.027.
- [21] K.H. Richards, N. Schanze, R. Monk, E. Rijntjes, D. Rathmann, J. Köhrle, A validated LC-MS/MS method for cellular thyroid hormone metabolism: Uptake and turnover of mono-iodinated thyroid hormone metabolites by PCCL3 thyrocytes, *PLoS One.* 12 (2017) e0183482. doi:10.1371/journal.pone.0183482.
- [22] D. Rathmann, E. Rijntjes, J. Lietzow, J. Köhrle, Quantitative Analysis of Thyroid Hormone Metabolites in Cell Culture

- Samples Using LC-MS/MS, *Eur. Thyroid J.* 4 (2015) 51–58. doi:10.1159/000430840.
- [23] L.M. Gonçalves, M.M. Moreira, C.F. Azevedo, I.M. Valente, J.C. Sousa, T.S. Scanlan, R.G. Compton, J.A. Rodrigues, Proof of Concept of the Electrochemical Sensing of 3-Iodothyronamine (T1AM) and Thyronamine (T0AM), *ChemElectroChem.* 1 (2014) 1623–1626. doi:10.1002/celec.201402165.
- [24] Z.-M. Li, F. Giesert, D. Vogt-Weisenhorn, K.M. Main, N.E. Skakkebaek, H. Kiviranta, J. Toppari, U. Feldt-Rasmussen, H. Shen, K.-W. Schramm, M. De Angelis, Determination of thyroid hormones in placenta using isotope-dilution liquid chromatography quadrupole time-of-flight mass spectrometry, *J. Chromatogr. A.* 1534 (2018) 85–92. doi:10.1016/j.chroma.2017.12.048.
- [25] M.E. Hart, K.L. Suchland, M. Miyakawa, J.R. Bunzow, D.K. Grandy, T.S. Scanlan, Trace Amine-Associated Receptor Agonists: Synthesis and Evaluation of Thyronamines and Related Analogues, *J. Med. Chem.* 49 (2006) 1101–1112. doi:10.1021/jm0505718.
- [26] G. Chiellini, G. Nesi, M. Digiacoimo, R. Malvasi, S. Espinoza, M. Sabatini, S. Frascarelli, A. Laurino, E. Cichero, M. Macchia, R.R. Gainetdinov, P. Fossa, L. Raimondi, R. Zucchi, S. Rapposelli, Design, Synthesis, and Evaluation of Thyronamine Analogues as Novel Potent Mouse Trace Amine Associated Receptor 1 ( m TAAR1) Agonists, *J. Med. Chem.* 58 (2015) 5096–5107. doi:10.1021/acs.jmedchem.5b00526.
- [27] S. Ghirmai, E. Mume, H. Lundqvist, V. Tolmachev, S. Sjöberg, Synthesis and radioiodination of some 9-aminoacridine derivatives for potential use in radionuclide therapy, *J. Label. Compd. Radiopharm.* 48 (2005) 855–871. doi:10.1002/jlcr.960.
- [28] L.F. Ferreira, C.C. Santos, F.S. da Cruz, R.A.M.S. Correa, R.M. Verly, L.M. Da Silva, Preparation, characterization, and application in biosensors of functionalized platforms with poly(4-aminobenzoic acid), *J. Mater. Sci.* 50 (2015) 1103–1116. doi:10.1007/s10853-014-8667-4.
- [29] Y. Zhang, J. Wang, M. Xu, A sensitive DNA biosensor fabricated with gold nanoparticles/poly (p-aminobenzoic acid)/carbon nanotubes modified electrode, *Colloids Surfaces B Biointerfaces.* 75 (2010) 179–185. doi:10.1016/j.colsurfb.2009.08.030.
- [30] Y.T. Liu, J. Deng, X.L. Xiao, L. Ding, Y.L. Yuan, H. Li, X.T. Li, X.N. Yan, L.L. Wang, Electrochemical sensor based on a poly(para-aminobenzoic acid) film modified glassy carbon electrode for the determination of melamine in milk, *Electrochim. Acta.* 56 (2011) 4595–4602. doi:10.1016/j.electacta.2011.02.088.
- [31] F. Lopes, J.G. Pacheco, P. Rebelo, C. Delerue-Matos, Molecularly imprinted electrochemical sensor prepared on a screen printed carbon electrode for naloxone detection, *Sensors Actuators B Chem.* 243 (2017) 745–752. doi:10.1016/j.snb.2016.12.031.
- [32] L. Yang, B. Xu, H. Ye, F. Zhao, B. Zeng, A novel quercetin electrochemical sensor based on molecularly imprinted poly( para -aminobenzoic acid) on 3D Pd nanoparticles-porous graphene-carbon nanotubes composite, *Sensors Actuators B Chem.* 251 (2017) 601–608. doi:10.1016/j.snb.2017.04.006.
- [33] M. Torkashvand, M.B. Gholivand, F. Taherkhani, Fabrication of an electrochemical sensor based on computationally designed molecularly imprinted polymer for the determination of mesalamine in real samples, *Mater. Sci. Eng. C.* 55 (2015) 209–217. doi:10.1016/j.msec.2015.05.031.
- [34] L.M. Gonçalves, C. Batchelor-Mcauley, A.A. Barros, R.G. Compton, Electrochemical oxidation of adenine: A mixed adsorption and diffusion response on an edge-plane pyrolytic graphite electrode, *J. Phys. Chem. C.* 114 (2010) 14213–14219. doi:10.1021/jp1046672.
- [35] H. da Silva, J. Pacheco, J. Silva, S. Viswanathan, C. Delerue-Matos, Molecularly imprinted sensor for voltammetric detection of norfloxacin, *Sensors Actuators B Chem.* 219 (2015) 301–307. doi:http://dx.doi.org/10.1016/j.snb.2015.04.125.
- [36] C. Batchelor-McAuley, L.M. Gonçalves, L. Xiong, A.A. Barros, R.G. Compton, Controlling voltammetric responses by electrode modification; using adsorbed acetone to switch graphite surfaces between adsorptive and diffusive modes, *Chem. Commun.* 46 (2010) 9037–9039. doi:10.1039/c0cc03961f.
- [37] A. Shrivastava, V. Gupta, Methods for the determination of limit of detection and limit of quantitation of the analytical methods, *Chronicles Young Sci.* 2 (2011) 21–25. doi:10.4103/2229-5186.79345.
- [38] R.M. Ramos, L.M. Gonçalves, V. Vyskočil, J.A. Rodrigues, Free sulphite determination in wine using screen-printed carbon electrodes with prior gas-diffusion microextraction, *Electrochem. Commun.* 63 (2016) 52–55. doi:10.1016/j.elecom.2015.12.010.

**Figure 1** – Chemical synthetic strategies followed for the obtention of T<sub>0</sub>AM (red route) and T<sub>1</sub>AM (blue route).

**Figure 2** – Schematic illustration of the construction of the SPCE-MIP sensor. 1) electropolymerization; 2) template extraction; 3) selective analysis.

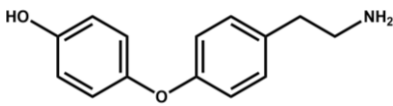
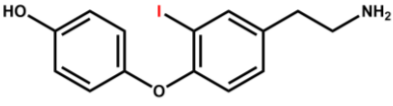
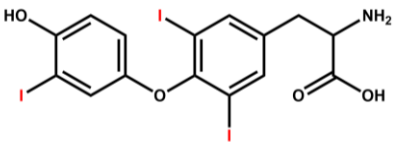
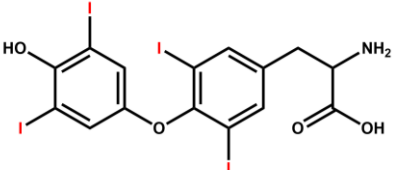
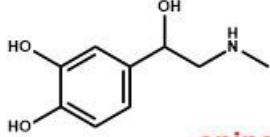
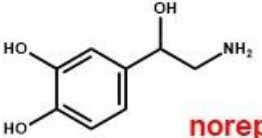
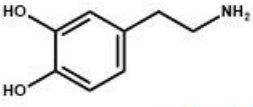
**Figure 3** - Characterization of the step by step construction of the sensor (4-ABA concentration of 10 mmol L<sup>-1</sup>, T<sub>0</sub>AM concentration of 1 mmol L<sup>-1</sup>, 10 minutes of incubation and hydrochloric acid/methanol as the extracting solvent): A) CV measurements performed over a 2 mmol L<sup>-1</sup> [Fe(CN)<sub>6</sub>]<sup>3-/4-</sup> in PBS, and B) the corresponding EIS Nyquist diagrams. a) SPCE; b) SPCE-NIP after polymerization; c) SPCE-MIP after polymerization; d) SPCE-MIP after template extraction; e) SPCE-MIP after incubation with T<sub>0</sub>AM.

**Figure 4** – Optimization of the electropolymerization conditions, all measurements were performed by SWV after incubation with a 40 µL drop of T<sub>0</sub>AM, 10 µmol L<sup>-1</sup>: A) Variation of the peak current with the concentration of monomer 4-ABA (T<sub>0</sub>AM template concentration was kept at 1 mmol L<sup>-1</sup>, the incubation time at 10 min., and the extraction solvent was hydrochloric acid/methanol, 50:50); B) Variation of the peak current with the concentration of the template molecule T<sub>0</sub>AM (4-ABA concentration was kept at 10 mmol L<sup>-1</sup>, the incubation time at 10 min., and the extraction solvent was hydrochloric acid/methanol, 50:50); C) Variation of the peak current with the incubation time (4-ABA concentration was kept at 10 mmol L<sup>-1</sup>, the T<sub>0</sub>AM template concentration was kept at 1 mmol L<sup>-1</sup>, and the extraction solvent was hydrochloric acid/methanol, 50:50); D) Variation of the peak current with the extraction solvent used (4-ABA concentration was kept at 10 mmol L<sup>-1</sup>, T<sub>0</sub>AM template concentration was kept at 1 mmol L<sup>-1</sup> and the incubation time at 10 min.). Hydrochloric acid concentration was 0.1 mol L<sup>-1</sup>, the ratios hydrochloric acid/methanol and water/dimethyl sulfoxide were both 50:50 (v/v).

**Figure 5** – A) Square-wave voltammograms in PBS of the SPCE-MIP, just before and right after removing the template by solvent extraction; B) Square-wave voltammograms in PBS after analyte incubation (T<sub>0</sub>AM, 1 mmol L<sup>-1</sup>, during 10 min.) in the unmodified SPCE, the NIP and the MIP.

**Figure 6** – Square-wave voltammograms of different T<sub>0</sub>AM concentrations, from 0.05 to 10 µmol L<sup>-1</sup>, in PBS. Inlay the corresponding calibration curve (each concentration was done in triplicate).

**Table 1** – Selectivity data, all compounds were analyzed with a concentration of 10  $\mu\text{mol L}^{-1}$

compound	$i_{p(MIP)} / \mu\text{A}$	$i_{p(NIP)} / \mu\text{A}$	IF	$\alpha$
 <p><b>T<sub>0</sub>AM</b></p>	3.160 ± 0.080	0.259 ± 0.080	10.0 ± 1.6	-
 <p><b>T<sub>1</sub>AM</b></p>	1.28 ± 0.12	0.644 ± 0.046	1.84 ± 0.21	5.4 ± 1.1
 <p><b>T<sub>3</sub></b></p>	0.145 ± 0.028	0.1273 ± 0.0093	1.14 ± 0.24	8.7 ± 2.3
 <p><b>T<sub>4</sub></b></p>	< LOD	< LOD	-	-
 <p><b>epinephrine</b></p>	0.287 ± 0.063	0.105 ± 0.038	2.7 ± 1.2	3.7 ± 1.7
 <p><b>norepinephrine</b></p>	0.442 ± 0.044	0.342 ± 0.034	1.29 ± 0.86	7.7 ± 1.7
 <p><b>dopamine</b></p>	0.53 ± 0.17	0.589 ± 0.059	0.89 ± 0.30	11.2 ± 4.2



## Highlights

- First time a sensor was developed for T<sub>0</sub>AM (thyronamine);
- Electroanalytical methodology for T<sub>0</sub>AM;
- Molecularly imprinted polymers (MIPs) were developed for T<sub>0</sub>AM;
- MIPs' polymerization (4-aminobenzoic acid to a poly(4-aminobenzoic acid) film) occurred in the surface of screen-printed carbon electrodes (SPCEs);
- The SPCE-MIP selectively analysed T<sub>0</sub>AM by square-wave voltammetry (SWV).

